

Supersonic Flutter of Laminated Curved Panels

M. Ganapathi

Institute of Armament Technology, Pune-411 025

and

T.K. Varadan

Department of Aerospace Engineering, Indian Institute of Technology, Madras-600 036

ABSTRACT

Supersonic flutter analysis of laminated composite curved panels is investigated using doubly-curved, quadrilateral, shear flexible, shell element based on field-consistency approach. The formulation includes transverse shear deformation, in-plane and rotary inertias. The aerodynamic force is evaluated using two-dimensional static aerodynamic approximation for high supersonic flow. Initially, the model developed here is verified for the flutter analysis of flat plates. Numerical results are presented for isotropic, orthotropic and laminated anisotropic curved panels. A detailed parametric study is carried out to observe the effects of aspect and thickness ratios, number of layers, lamination scheme, and boundary conditions on flutter boundary.

NOMENCLATURE

$2a, 2b$	Shell panel dimensions	K	Stiffness matrix
A_1	Aerodynamic matrix	K_{cr}^2	Critical flutter frequency ($=\omega^2 a^4 \rho h/D$)
$A_{i,j}$ ($i,j = 1,2,3$)	Elements of extensional stiffness matrix	M	Mass matrix
$B_{i,j}$ ($i,j = 1,2,3$)	Elements of bending-extensional coupling matrix	M_∞	Free stream Mach number
D	$Eh^3/12(1-\nu^2)$	M_{xx}, M_{yy}, M_{xy}	Bending stress resultants
\bar{D}_{11}	$E_L h^3/12(1-\nu_{LT} \nu_{TT})$	N_x^0, N_y^0, N_{xy}^0	Applied in-plane stresses
$D_{i,j}$ ($i,j = 1,2,3$)	Elements of bending stiffness matrix	N_{xx}, N_{yy}, N_{xy}	Membrane stress resultants
E	Young's modulus	\bar{N}_x, \bar{N}_y	Non-dimensional applied in-plane stresses ($=N_x^0 a^2/\pi^2 D, N_y^0 a^2/\pi^2 \bar{D}$)
E_L, E_T	Young's moduli in the longitudinal and transverse directions	Q_{xz}, Q_{yz}	Transverse shear forces
E_r	Reference modulus	R	Radius of cylindrical panel
$E_{i,j}$ ($i,j = 4,5$)	Elements of shear stiffness matrix	R_x, R_y	Radii of curvature in x, y directions
G_{LT}, G_{TT}	Shear moduli of a lamina in the in-plane and transverse directions	t	Time
h	Shell thickness	T	Kinetic energy
k_1^2, k_2^2	Shear correction factors	U	Strain energy
		U_a	Free stream velocity
		u_0, v_0	Mid-plane displacements
		u, v, w	Displacements

W	Work done by the applied non-conservative force
$x, y, z,$	Coordinates
Δp	Aerodynamic pressure developed over small element
β	Aerodynamic pressure parameter ($= \rho_a U_a^2 / \sqrt{M_\infty^2 - 1}$)
	Critical aerodynamic pressure parameter and pressure ($\lambda_{cr} = \beta a^3 / E_r h^3$)
	Critical aerodynamic pressures ($= \beta a^3 / D, \beta a^3 / \bar{D}_{11}$)
$\epsilon_p, \epsilon_b, \epsilon_s$	Mid-plane strains, bending curvatures and shear strains
ϕ	Angle
ν	Poisson's ratio for isotropic material
ν_{LT}, ν_{TT}	Poisson's ratio for orthotropic material
θ_x, θ_y	Rotations
ρ	Mass density of material
ρ_a	Mass density of air
ω	Natural frequency
ω_r, ω_i	Real and imaginary part of frequency
$\bar{\omega}^2$	Non-dimensional frequency ($= \omega^2 a^4 \rho / E_L h^2$)
ω_f	Flutter frequency
σ	Initial stress matrix
$(), x$	Partial derivative with respect to x
	Derivative with respect to time
$($	Symmetric layers.

INTRODUCTION

A panel supported on an elastic medium often finds application in the construction of aerospace/missile structures. During high speed flight, the external skin of the panel of an airframe may experience flutter which sometimes may cause destructive damage to the structure of the flight vehicle. Panel flutter is a self-excited oscillation of the external skin of a flight vehicle and is due to dynamic instability caused by the interaction of inertia, elastic and aerodynamic forces of the system. Study of such aeroelastic instability of flat/curved plates is very important in aerospace structural design in evaluating the fatigue life and allowable cyclic stress of these components exposed to supersonic flow. Linear flutter analyses of flat isotropic

plates have received considerable attention in the literature and have been reviewed by Dowell¹. Several attempts²⁻⁶ were made to solve analytically the non-linear flutter behaviour of plates. The dynamic instability of flutter of isotropic flat plates was also investigated through many finite element formulations⁷⁻¹²

Nowadays composite materials play an increasing role in aircraft industry. Aeroelastic tailoring of flight vehicle structures which has a great potential to improve the performance has attracted substantial attention recently.

The influence of orthotropic properties on critical flutter speed of flat plates was studied by several authors¹³⁻¹⁶. Sawyer¹⁷, using classical lamination theory, investigated the flutter analysis of laminated plates. It is revealed that couplings of bending-stretching and bending-twisting produce a destabilising effect on buckling and flutter. Birman and Librescu¹⁸ have presented an analytical model based on shear flexible theory for the study of flutter characteristics of laminated plates. Srinivasan and Babu¹⁹ examined the flutter of laminated quadrilateral plates. However, the flutter behaviour of isotropic/composite curved plates, in general, was treated sparsely in the literature²⁰⁻²⁴. In Ref. 24, availing classical shell theory, critical aerodynamic pressures have been evaluated using integral equation technique. Finite element techniques have been used to evaluate the critical aerodynamic pressure for laminated anisotropic flat plates²⁵⁻²⁷. These techniques, however, have not found their applications to curved plates.

Effect of shear deformation, depending on geometrical and material properties, plays a significant role in determining the global characteristics. For isotropic material, shear deformation and rotary inertia effects can be neglected when the structure is thin. However, in the case of laminated composites, where the ratio of in-plane modulus to shear modulus is generally high, these effects cannot be neglected even if the structure is thin. For example, results presented in the recent work due to Birman and Librescu¹⁸ reveal considerable transverse shear deformation effects on supersonic flutter of advanced composite flat panels.

Hence it is preferable to use a shear flexible theory when one thinks of analysis of laminated structures by the finite element method. To extend such a formulation

for thin shell, reduced/selective integration technique is generally employed to eliminate spurious energy due to membrane/shear locking. Finite elements based on field-consistency principle, developed recently for the structural analysis of thick as well as thin plates/shells²⁸, do not exhibit locking phenomenon and do not require the reduced/selective integration technique. The performance of such an element for dynamic studies has not yet been examined.

In the present work, eight-noded serendipity-type doubly-curved, shear flexible element, based on field-consistency principle²⁸ is used for analysing the dynamic instability of laminated anisotropic curved panels in supersonic flow. The non-conservative aerodynamic forces are evaluated using a first-order, high Mach number approximation to the linear potential flow theory. The numerical results are obtained for isotropic, orthotropic and laminated anisotropic panels. Wherever possible, comparison is made with the existing solutions. A detailed study is made to bring out the influence of number of layers, ply angles, aspect ratios, radius-to-side ratios, side-to-thickness ratios and boundary conditions.

2. FORMULATION

A doubly-curved laminated composite shell is considered with the coordinates x, y along the in-plane directions and z along the radial/thickness direction. Using Mindlin formulation, the displacements u, v, w at a point (x, y, z) from the median surface are expressed as functions of mid-plane displacements u_0, v_0 and w , and independent rotations θ_x and θ_y of the normal in xz and yz planes respectively, as

$$\begin{aligned} u(x, y, z, t) &= u_0(x, y, t) + z\theta_x(x, y, t) \\ v(x, y, z, t) &= v_0(x, y, t) + z\theta_y(x, y, t) \\ w(x, y, z, t) &= w_0(x, y, t) + z\theta_z(x, y, t) \end{aligned} \quad (1)$$

The strains in terms of mid-plane deformation of Eqn (1) for a shell, based on Novozhilov's theory, are given as

$$\{\epsilon\} = \begin{Bmatrix} \epsilon_p \\ 0 \end{Bmatrix} + \begin{Bmatrix} z\epsilon_b \\ \epsilon_s \end{Bmatrix} \quad (2)$$

The mid-plane strains ϵ_p , bending strains ϵ_b , and shear strains ϵ_s in Eqn (2) are written as

$$\begin{aligned} \{\epsilon_p\} &= \begin{Bmatrix} u_{0,x} + (w/R_x) \\ v_{0,y} + (w/R_y) \\ u_{0,y} + v_{0,x} \end{Bmatrix} \\ \{\epsilon_b\} &= -\begin{Bmatrix} \theta_{x,x} \\ \theta_{y,y} \\ \theta_{x,y} + \theta_{y,x} - (u_{0,y}/R_x) - (v_{0,x}/R_y) \end{Bmatrix} \\ \{\epsilon_s\} &= \begin{Bmatrix} \theta_x - w_{,x} + (u_0/R_x) \\ \theta_y - w_{,y} + (u_0/R_y) \end{Bmatrix} \end{aligned}$$

where R_x and R_y are the usual radii of curvatures.

If $\{N\}$ represents the membrane stress resultants (N_{xx}, N_{yy}, N_{xy}) and $\{M\}$ the bending stress resultants (M_{xx}, M_{yy}, M_{xy}), one can relate these to membrane strains $\{\epsilon_p\}$ consisting of linear and nonlinear components and bending strains $\{\epsilon_b\}$ through the constitutive relations as

$$\begin{aligned} \{N\} &= [A_{ij}] \{\epsilon_p\} + [B_{ij}] \{\epsilon_b\} \quad \text{and} \\ \{M\} &= [B_{ij}] \{\epsilon_p\} + [D_{ij}] \{\epsilon_b\} \end{aligned} \quad (3)$$

where A_{ij}, D_{ij} and B_{ij} ($i, j = 1, 2, 3$) are extensional, bending, and bending-extensional stiffness coefficients of the composite laminate. Similarly, the transverse shear force $\{Q\}$ representing the quantities (Q_{xz}, Q_{yz}) are related to the transverse shear strains $\{\epsilon_s\}$ through the constitutive relations as

$$\{Q\} = [E_{ij}] \{\epsilon_s\} \quad (4)$$

where E_{ij} ($i, j = 4, 5$) are the transverse shear stiffness coefficients of the laminate.

For a composite laminate of thickness h , consisting of N layers with stacking angles ϕ_i ($i = 1, N$) and layer thickness h_i ($i = 1, N$), the necessary expressions to compute the stiffness coefficients, available in the literature²⁹ are used here. The strain energy functional U is given by

$$\begin{aligned} U(\delta) &= \frac{1}{2} \int_A [\{\epsilon_p\}^T [A_{ij}] \{\epsilon_p\} \\ &\quad + \{\epsilon_p\}^T [B_{ij}] \{\epsilon_b\} + \\ &\quad + \{\epsilon_b\}^T [B_{ij}] \{\epsilon_p\} + \{\epsilon_b\}^T [D_{ij}] \{\epsilon_b\} + \\ &\quad + \{\epsilon_s\}^T [E_{ij}] \{\epsilon_s\}] dA \end{aligned} \quad (5)$$

where δ is vector of degrees of freedom

The kinetic energy of the shell is given by

$$T(\delta) = \frac{1}{2} \int_A [\rho (\dot{u}^2 + \dot{v}^2 + \dot{w}^2) + I(\theta_x^2 + \theta_y^2)] dA \quad (6)$$

where $p = \int_0^h \rho dz$, $I = \int_0^h z^2 \rho dz$ and ρ is mass density.

The panel is subjected to in-plane stress resultant per unit length N_x^0 , N_y^0 , and N_{xy}^0 , respectively. The potential energy due to the applied conservative loads is

$$V(\delta) = \frac{1}{2} \int_A [N_x^0 w_x^2 + N_y^0 w_y^2 + 2N_{xy}^0 w_x w_y] dA \quad (7)$$

The work done by the applied non-conservative loads is

$$W(\delta) = \int_A \Delta p w dA \quad (8)$$

where Δp is the aerodynamic pressure. The aerodynamic pressure for high supersonic speed, within the 2-D static approximation^{18,30} is given as

$$\Delta p = -\frac{\rho_a U_a^2}{\sqrt{M_\infty^2 - 1}} \frac{\partial w}{\partial x} \quad (8a)$$

where ρ_a , U_a , and M are free stream air density, free stream velocity and Mach number, respectively. As has been shown previously³⁰, the two-dimensional static aerodynamic approximation provides results that are in complete agreement with those based on exact aerodynamic theories for Mach numbers between $\sqrt{2}$ and 2. Substituting Eqns (5)-(8) in Lagrange's equation of motion, one obtains the governing equation for the curved panel as

$$[M] \{\delta\} + [\beta[A1] + [K] + [\sigma]] \{\delta\} = 0$$

where $[M]$ and $[A1]$ are the mass and aerodynamic matrices, respectively; $[K]$ and $[\sigma]$ are stiffness and initial stress matrices, and β is the aerodynamic pressure parameter defined as

$$\frac{\rho_a U_a^2}{\sqrt{M_\infty^2 - 1}} \quad (9)$$

Introducing a harmonic motion in the $\{\delta\} = \{\delta_0\} e^{i\omega t}$ Eqn (9) is rewritten as

$$[\bar{K}] - \omega^2 [M] \{\delta_0\} = 0$$

where $[\bar{K}] = [K] + [\sigma] + \beta [A1]$, and ω is the natural frequency.

Now the problem is reduced to that of finding the eigen-values ω and corresponding mode shapes of the system for a given value of β . When $\beta > 0$, the eigen-value ω is real and positive definite, since $[\bar{K}]$ and $[M]$ are symmetric and positive definite. However, aerodynamic matrix $[A]$ is not symmetric and hence complex eigen-values ω are expected for $\beta > 0$. As β increases monotonically from zero, two of these eigen-values will approach each other and coalesce to ω_{cr} at $\beta = \beta_{cr}$ to and become complex conjugate pairs

$$\omega = \omega_r \pm i\omega_i$$

for $\beta > \beta_{cr}$. Here, β_{cr} corresponds to the value of ω at which first coalescence occurs.

3. ELEMENT DESCRIPTION

The laminated shell element considered here is a C^0 continuous shear flexible element and needs five nodal degrees of freedom, u , v , w , θ_x and θ_y at eight nodes in QUAD-8 element as shown in Fig. 1.

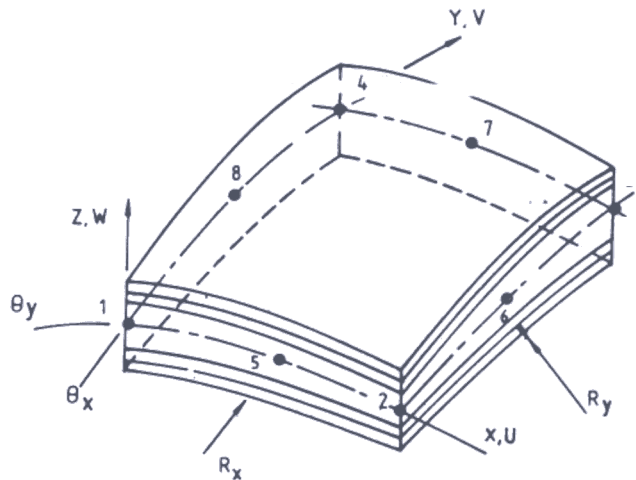


Figure 1 Geometry of a laminated curved shell.

If the interpolation functions for QUAD-8 are used directly to interpolate the five field variables u , v , w , θ_x and θ_y in deriving the shear and membrane strains,

the element will lock and show oscillations in the shear and membrane stresses. Field consistency requires that the transverse shear strains and membrane strains must be interpolated in a consistent manner. Thus u, v, θ_x and θ_y terms in the expression for $\{\epsilon_s\}$ given in Eqn (2c) have to be consistent with field functions w_x and w_y as shown in the work of Prathap, et al²⁸. Similarly w term in the expression for $\{\epsilon_p\}$ given in Eqn (2a) has to be consistent with field functions (u_x, v_y) and (u_y, v_x) . This is achieved by using field redistributed substitute shape functions to interpolate those specific terms which must be consistent as described by Prathap, et al²⁸

4. RESULTS AND DISCUSSION

Here we present results for isotropic, laminated orthotropic and anisotropic curved panels. All the computations are made using CYBER 180/840A processor with double precision arithmetic. All the energy terms are evaluated based on exact numerical integration scheme. The shear correction factor is taken as 5/6. The boundary conditions considered in the analysis are

Simply supported :

$$u = 0, v = 0, w = 0, \theta_y = 0 \text{ at } x = \pm a$$

$$u = 0, v = 0, w = 0, \theta_x = 0 \text{ at } y = \pm b$$

Clamped supports

$$u = 0, v = 0, w = 0, \theta_x = 0, \theta_y = 0 \text{ at } x = \pm a$$

and at $y = \pm b$ (12)

A convergence study is carried out for a simply-supported isotropic plate. It is seen from Table 1 that the results obtained with 4 x 4 mesh are in good agreement with exact solution⁷ and this mesh size is taken for subsequent studies. The capabilities of the model developed here are tested for the effects of axial compression and thickness on dynamic instability of flutter and the results are compared with available results in Table 2.

In Table 3, critical non-dimensional dynamic pressures for simply supported rectangular orthotropic flat plates of different aspect ratios ($a/b = 1,2,3$) are presented for both thin and moderately thick situations. The material properties used are as follows:

Table 1. Convergence study of a simply supported isotropic square plate

Mesh	$\bar{\lambda}_{cr}^0$	K_{cr}^2
2 x 2	532.34	1891.0
3 x 3	514.77	1856.5
4 x 4	512.85	1849.35
5 x 5	512.68	1848.5
Exact ⁷	512.65	1848.2

Table 2. Critical dynamic pressure $\bar{\lambda}_{cr}^0$ of isotropic simply supported plates

a/b	\bar{N}_x	\bar{N}_y	a/h	$\bar{\lambda}_{cr}^0$		
				Present study	Ref. 11	Ref. 10
0	0	0	100	343.48	343.3680	343.5
				(343.3564)		
			10	314.98	314.9926	
0	0	0	5	248.25	248.6016	
			100	265.73		265.0
-	0	0	100	512.85		512.334
			100	343.45		342.0

⁺Exact value³¹

Table 3. Critical dynamic pressure $\bar{\lambda}_{cr}$ of orthotropic simply supported plates

a/b	a/h = 100	Ref. 16	a/h = 10
	Present study		Present study
3	397.78		298.80
	507.18	-	376.62
	708.34	670 ⁺	511.29

⁺Value of (a/h) is not given except it is mentioned that the plate is thin.

$$\frac{E_L}{E_T} = 5.3545, \quad \frac{G_{LT}}{E_T} = 0.41, \quad \frac{G_{TT}}{E_T} = 0.2,$$

$$v_{LT} = v_{TT} = 0.2727$$

$$E_T = 10^6 \text{ psi } (6.8953 \times 10^{10} \text{ N/m}^2),$$

$$\rho = 1.4786 \times 10^{-4} \text{ lb-sec}^2/\text{in}^2 \text{ (1580.48 kg/m}^3\text{)} \quad (13)$$

where subscripts *L* and *T* refer to longitudinal and transverse directions respectively with respect to fibres. All the layers are of equal thickness.

A similar investigation is made for laminated anisotropic flat plates and the material properties chosen are as follows:

$$\frac{E_L}{E_T} = 10, \quad \frac{G_{LT}}{E_T} = 0.33, \quad \frac{G_{TT}}{E_T} = 0.15,$$

$$v_{LT} = v_{TT} = 0.3$$

$$E_T = 10^6 \text{ psi}, \quad \rho = 1.4786 \times 10^{-4} \text{ lb-sec}^2/\text{in}^4 \quad (14)$$

Results for thick and thin laminated plates are presented in Table 4. It can be noted that the results given in Ref. 17 are based on classical laminated plate theory.

For detailed analyses both thin and moderately thick panels of the following cases are considered:

- (i) Isotropic curved panels,
- (ii) A single-layered orthotropic curved panels, and
- (iii) Cross-ply and angle-ply curved panels.

The material properties, for the parametric study, are assumed as:

Isotropic case :

$$E_L = 13 \times 10^6 \text{ psi } (8.9647 \times 10^{10} \text{ N/m}^2), \quad \nu = 0.33$$

$$\rho = 8.33 \times 10^{-4} \text{ (lb-sec}^2/\text{in}^4\text{)} \text{ (8903.94 kg/m}^3\text{)}$$

Orthotropic/Laminated case :

$$(E_L/E_T) = 25, \quad (G_{LT}/E_T) = 0.5, \quad (G_{TT}/E_T) = 0.2,$$

$$E_L = 25 \times 10^6 \text{ psi}, \quad \rho = 1.4786 \times 10^{-4} \text{ lb-sec}^2/\text{in}^4 \quad (15)$$

Table 4. Critical dynamic pressure $\bar{\lambda}_{cr}$ of laminated four-layered simply supported plates

a/b	a/h	(-45°/45° / -45°/45°)		(0°/90° / 0°/90°)	
		Present study $\bar{N}_x = 0$	Ref. 17 $\bar{N}_x = 0$	Present study $\bar{N}_x = 0$	Ref. 17 $\bar{N}_x = 0$
2	100		222.7	54.6	
	10	160.60		44.75	
	100	684.06		141.88	
	10	282.25		58.39	

Plots of critical dynamic pressure and radius-to-side ratio for the two boundary conditions for the above cases, with different aspect ratios, lamination schemes, and side-to-thickness (*b/h*) are shown in Figs 2-5.

In Figs 2 and 3, for the selected values of *a/b* (1 and 2) and *b/h* (100,10) the variations of non-dimensional critical dynamic pressure, $\lambda_{cr}[\beta a^3/E_r h^3]$ with *R/b* for isotropic panel are shown. The reference modulus E_r used in the calculation is *E* for the isotropic case and E_L for the orthotropic/laminated case. It is observed, that for large values of (*R/b*) the flutter speed is not influenced by the radius of curvature. It has to be so as the curved panel geometry approaches the flat panel one and similar observations are made by Dowell²², Matsuzaki²³, and Srinivasan and Babu²⁴. However, it is found that the flutter boundary has peaks and abrupt drop-offs for the panel geometry of *R/b* = 1 to 4. This is due to frequency coincidence of

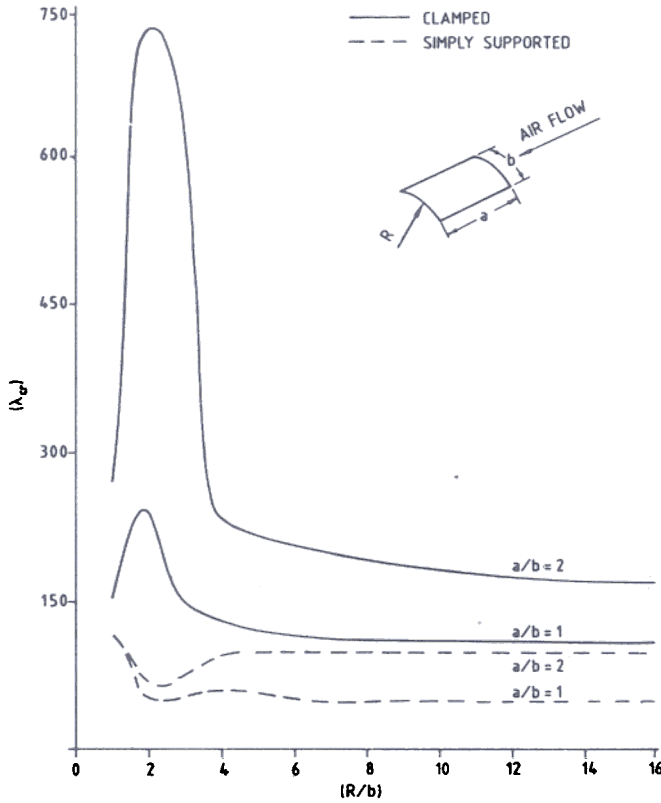


Figure 2. Critical dynamic pressure vs radius-to-side ratio for isotropic panels ($b/h = 100$).

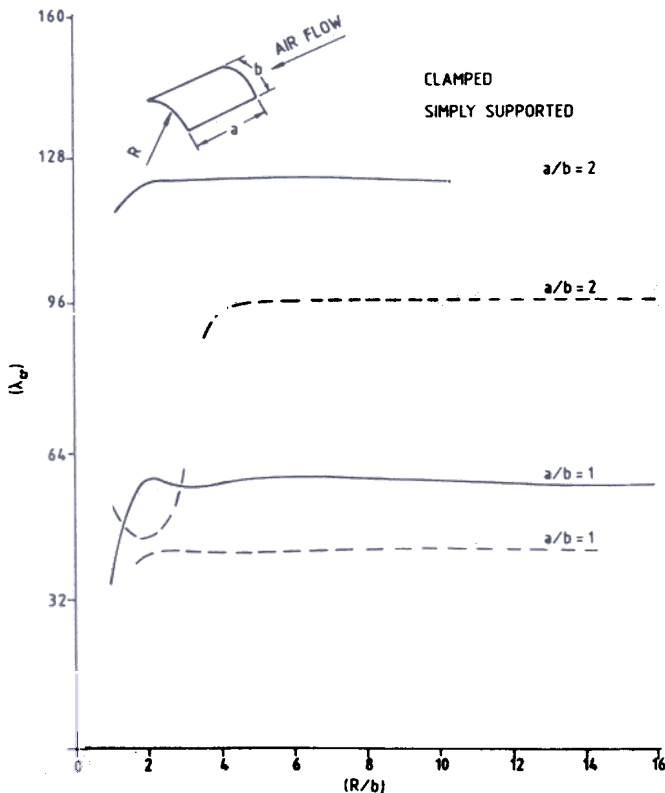


Figure 3. Critical dynamic pressure vs radius-to-side ratio for isotropic panels ($b/h = 10$).

aero-elastically related natural modes. Similar feature is highlighted by Matsuzaki²³. The boundary conditions imposed on shell geometry play a significant role in determining the flutter boundary as reported in literature²⁰⁻²³. When the curved panels fall into the category of deep panels, it is seen that the boundary conditions affect the flutter behaviour qualitatively. The actual critical flutter boundary increases with increase in aspect ratio and thickness. It is also inferred during the stability analysis that the coalescences of higher modes jump to the lower modes when the structure becomes shallow. In general, the panel with clamped conditions is stronger against flutter instability than the simply supported one.

Similar investigations are carried out for the cylindrical panel made of orthotropic materials and the flutter characteristics are drawn in Figs 4 and 5. They also predict, in general, qualitatively the same behaviour as that of an isotropic shell.

For a selected geometry and material properties, and clamped boundary condition, the variation of non-dimensional dynamic pressure with R/b for varying E_L/E_T (E_L is kept as a constant, equal to 25×10^6 psi and E_T alone is varied) is shown in Fig. 6 to bring out the effect of orthotropy. When $R/b > 6$, the critical dynamic pressure goes down by approximately a factor of 2 compared to the isotropic case ($E = E_L = 25 \times 10^6$ psi). For $R/b < 6$, the critical dynamic pressure decreases drastically when the orthotropy $E_L/E_T = 10, 25$ and 40 are introduced. Table 5 presents the non-dimensional natural frequency parameters (in vacuo) and flutter parameters (coalescence) for the above-mentioned cases ($E_L/E_T = 1, 10, 25$ and 40). It may be noted from Table 5 that both frequencies and flutter speed decrease when the orthotropicity is introduced, and in particular as E_T is decreased.

Laminated anisotropic curved panels with the following combinations of ply-angles and number of layers are now considered:

- Cross-ply : Two-layered panels ($0^\circ/90^\circ$)
- Three-layered panels ($0^\circ/90^\circ/0^\circ$)
- Eight-layered panels ($0^\circ/90^\circ/0^\circ/90^\circ$),
- Angle-ply : Two-layered panels ($45^\circ/-45^\circ$)
- Three-layered panels ($45^\circ/-45^\circ/45^\circ$)
- Eight-layered panels ($45^\circ/-45^\circ/45^\circ/-45^\circ$),

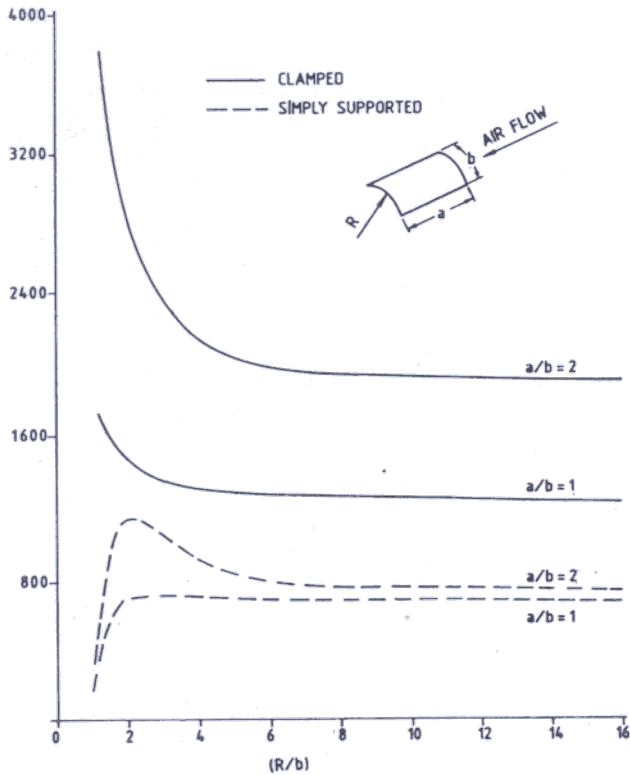


Figure 4. Critical dynamic pressure vs radius-to-side ratio for orthotropic panels ($b/h = 100$).

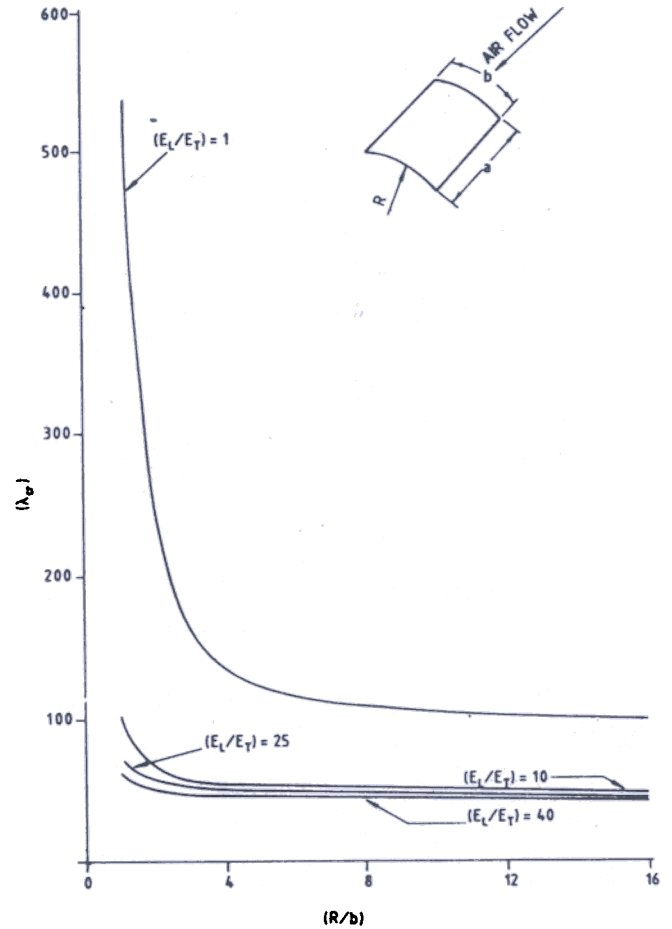


Figure 6. Critical dynamic pressure vs radius-to-side ratio for orthotropic panels. ($a/b = 1, b/h = 100, G_{LT}/E_T = 0.5, G_{TT}/E_T = 0.2, E_L = E = 25 \times 10^6$ psi, $\nu_{LT} = \nu_{TT} = \nu = 0.25, \rho = 1.4786 \times 10^{-4}$ lb-sec²/in⁴)

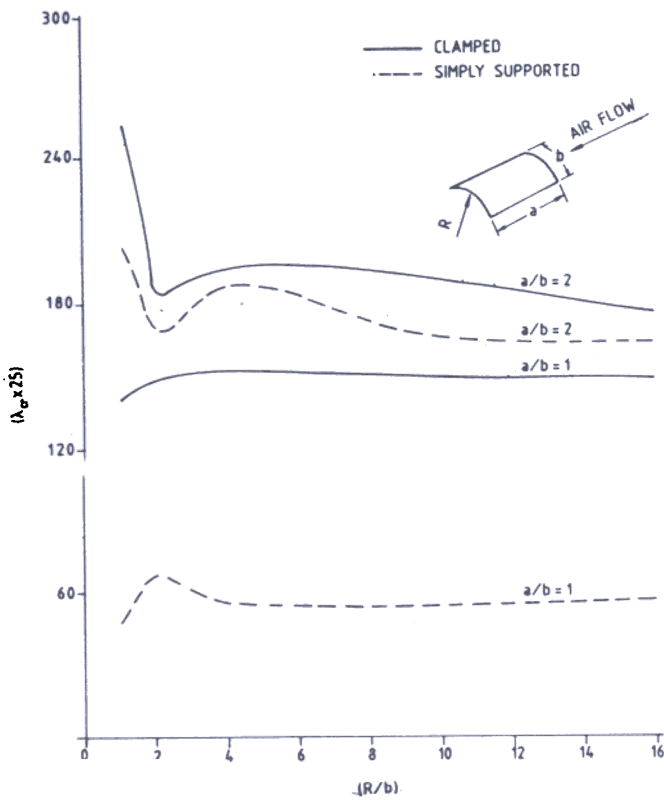


Figure 5. Critical dynamic pressure vs radius-to-side ratio for orthotropic panels ($b/h = 10$).

Ply-angle is measured from longitudinal axis of panel in the anti-clockwise direction. The first layer corresponds to the outermost layer and all the layers are of equal thickness.

The non-dimensional critical aerodynamic pressure is plotted against radius-to-side ratio in Figs 7-10 for cross-ply panels of different aspect ratios and side-to-thickness ratios. For fairly large values of (R/b) , three layer cross-ply panel predicts higher values of flutter speeds compared to that of two- and eight-layered cross-ply panels. This is because the directional stiffness provided by three-layered cross-ply is high against the airflow. Due to bending-stretching coupling, the panel with two layers offers less resistance against flutter than that of three- and eight-layered panels. It is observed that for deep panels, the flutter boundary is affected qualitatively by the number of layers in the panel and

Table 5. Non-dimensional natural frequencies and coalescence values of clamped square orthotropic panels

Material	Non-dimensional frequency (in vacuo)	Non-dimensional frequency		Coalescence		Coalescence mode		
		$\bar{\omega}_1^2$	$\bar{\omega}_2^2$	$\bar{\omega}_1^2$	λ_{cr}			
10	E_L/E_T	R/b	$\bar{\omega}_1^2$	$\bar{\omega}_2^2$	$\bar{\omega}_1^2$	λ_{cr}	Coalescence mode	
			803.6	2644.1	3716.1	2734.4	.20	(1,2)
			230.3	974.1	2222.5	798.2	.77	(1,2)
			162.0	788.2	2112.2	595.4	.44	(1,2)
			131.6	696.6	2056.6	511.5	.40	(1,2)
			121.2	667.6	2029.5	483.9	.52	(1,2)
			142.0	468.0	632.5	598.6	100.20	(2,3)
			63.8	295.9	467.9	357.1	56.64	(2,3)
			54.9	284.0	384.8	347.0	53.62	(2,3)
			50.9	279.1	374.8	329.6	51.79	(2,3)
25			49.5	277.5	371.5	326.9	47.80	(2,3)
			80.9	213.0	420.5	340.9	71.09	(2,3)
			48.7	145.6	328.1	241.3	53.91	(2,3)
			45.1	140.2	319.0	231.7	52.34	(2,3)
			43.5	138.3	315.0	227.5	50.95	(2,3)
			42.9	137.7	313.7	226.2	46.60	(2,3)
			63.8	146.2	349.9	275.4	60.94	(2,3)
			43.8	163.8	292.8	215.0	48.82	(2,3)
40			41.6	100.9	287.2	209.5	48.04	(2,3)
			40.6	99.7	284.8	204.6	47.50	(2,3)
			40.3	99.3	283.9	198.5	46.50	(2,3)

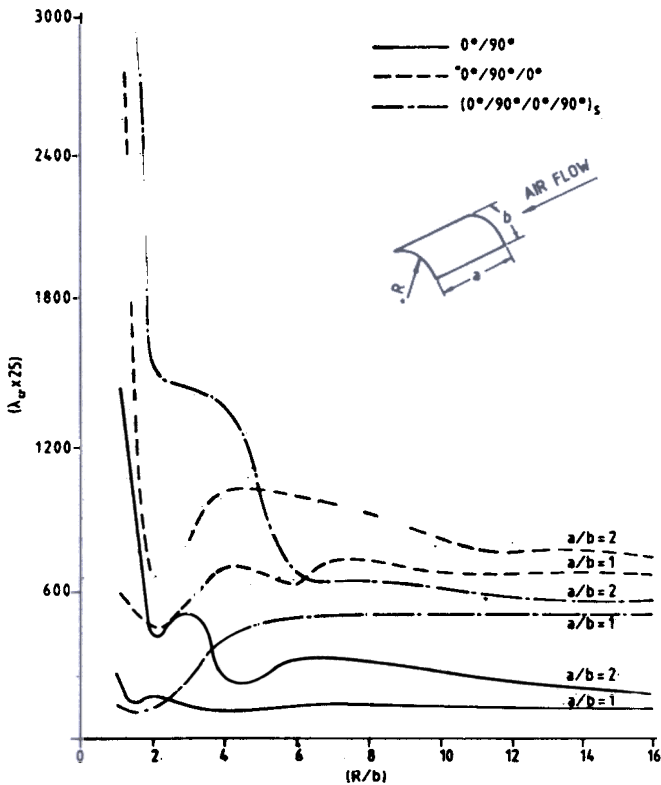


Figure 7. Critical dynamic pressure vs radius-to-side ratio for multilayered cross-ply panels with simply supported boundary condition ($b/h = 100$).

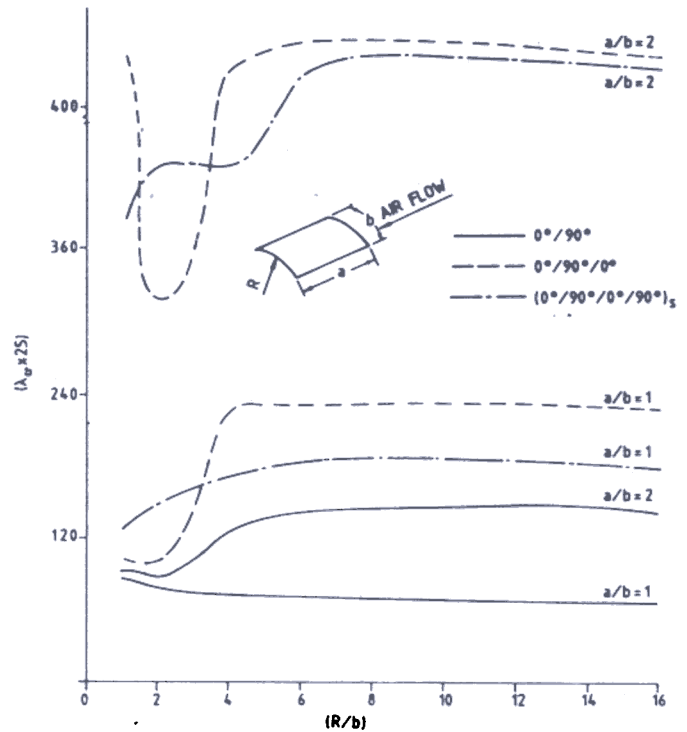


Figure 8. Critical dynamic pressure vs radius-to-side ratio for multilayered cross-ply panels with simply supported boundary condition ($b/h = 10$).

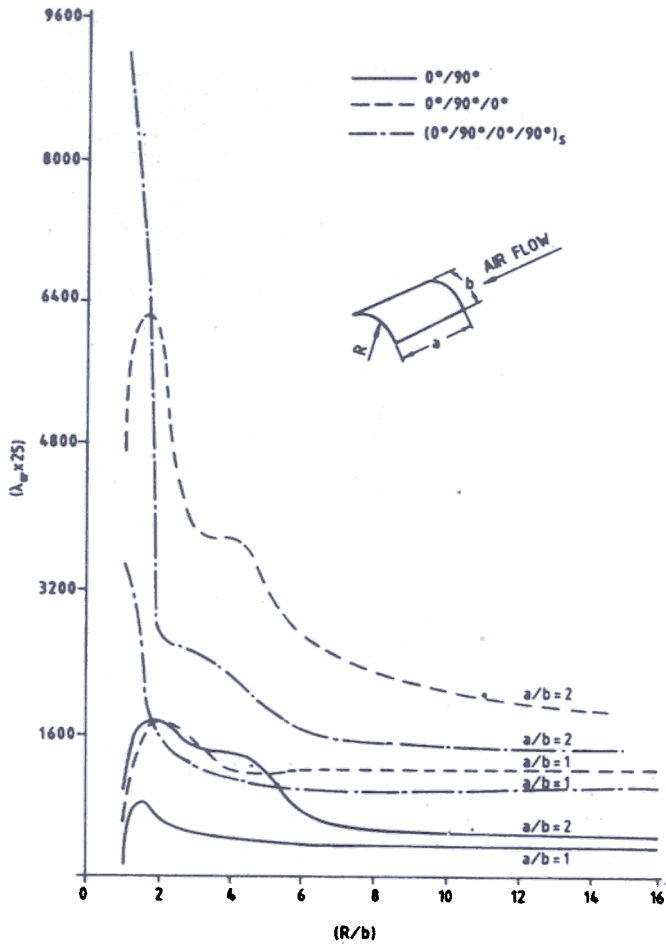


Figure 9. Critical dynamic pressure vs radius-to-side ratio for multilayered cross-ply panels with clamped boundary condition ($b/h = 100$).

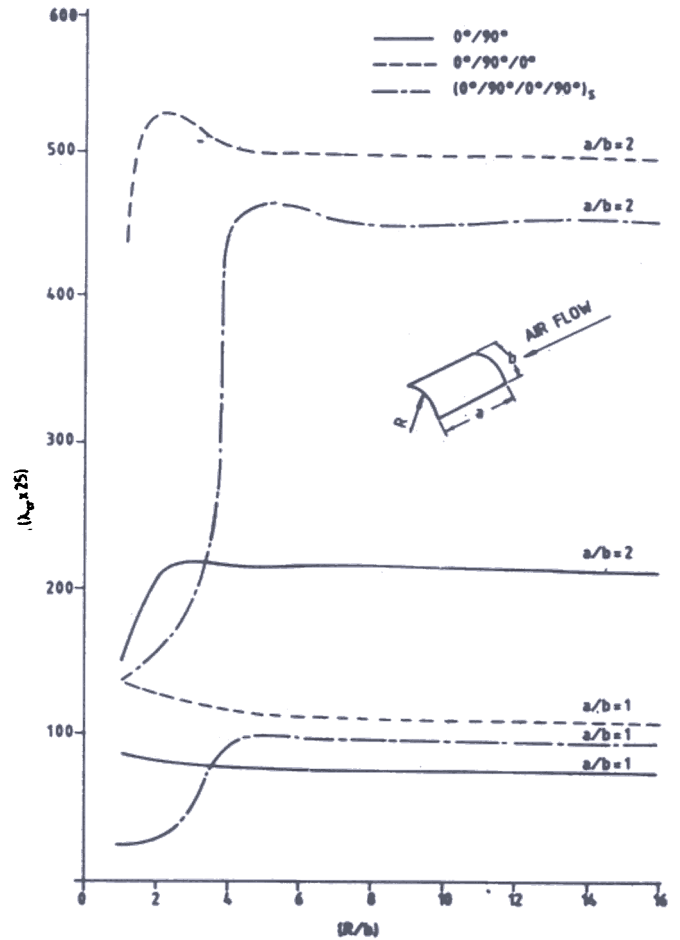


Figure 10. Critical dynamic pressure vs radius-to-side ratio for multilayered cross-ply panels with clamped boundary condition ($b/h = 10$).

to a lesser extent by the boundary conditions. The variation of critical flutter speed against radius-to-side ratios for angle-ply of different aspect ratios and thickness ratios are shown in Figs. 11-14. It is noticed from these figures that the critical flutter speed increases with increase in number of layers. The bending-twisting and stretching-shear coupling effects reduce the flutter speed significantly. Boundary conditions in deep panels affect the flutter characteristics qualitatively, like cross-ply panels. In thick shallow ($R/b > 4$) panel with increase in the aspect ratio, the predicted flutter boundary increases very much with number of layers compared to that of thin panels. This observation is found to be true for the boundary conditions and ply-orientations investigated here. Clamped panels produce higher critical values than the simply supported ones do. As in isotropic/orthotropic panel, increase in thickness and aspect ratios will increase the critical

aerodynamic pressure, and coalescence of higher modes is observed with increase in the curvature of the panel. In the light of the present findings, it is worthwhile to carry out an experimental study for the panel geometry with R/b in the range of 1-4, to confirm the curvature effect on flutter speed.

5. CONCLUSIONS

The effectiveness of an eight-noded, quadrilateral, shear flexible, shell element based on field-consistency principle is demonstrated for the first time, for dynamic analysis by studying the flutter behaviour of thin/thick laminated anisotropic cylindrical panels, exposed to supersonic flow field. Since the element is based on field-consistency approach, all the energy terms are evaluated with exact numerical integration scheme. It is found that flutter characteristics are strongly

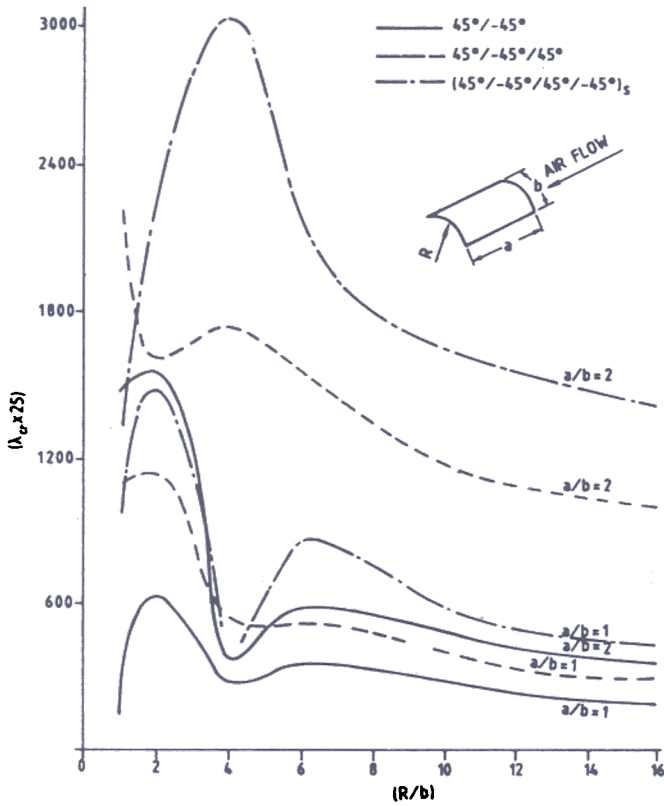


Figure 11. Critical dynamic pressure vs radius-to-side ratio for multilayered angle-ply panels with simply supported boundary condition ($b/h = 100$).

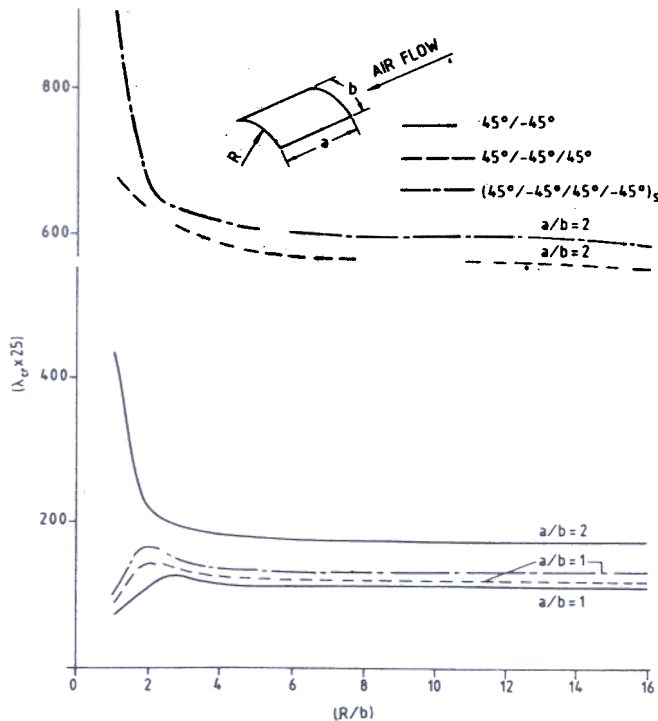


Figure 12. Critical dynamic pressure vs radius-to-side ratio for multilayered angle-ply panels with simply supported boundary condition ($b/h = 10$).

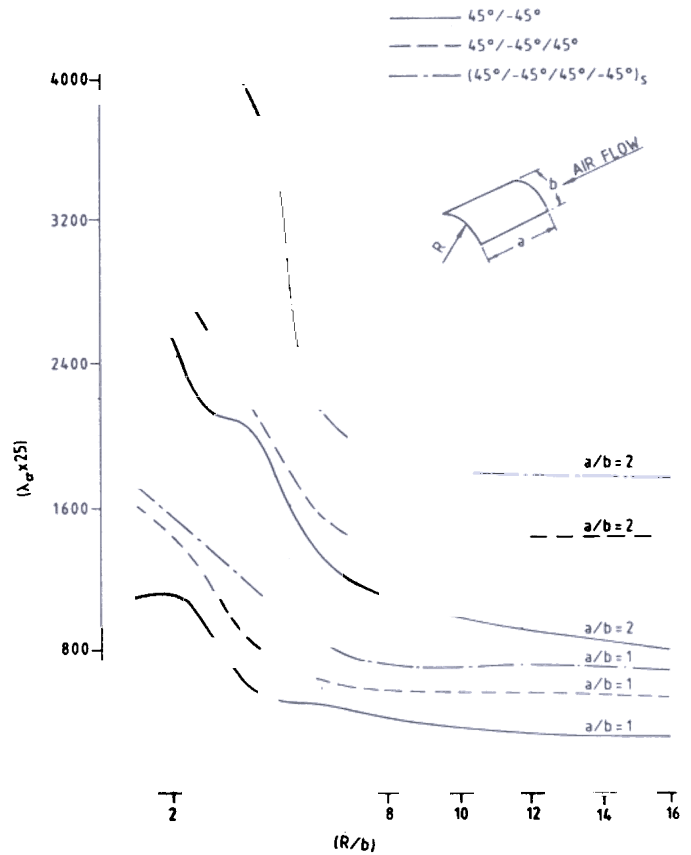


Figure 13. Critical dynamic pressure vs radius-to-side ratio for multilayered angle-ply panels with clamped boundary condition ($b/h = 100$).

controlled by directional stiffness provided by the anisotropic properties of laminated panels. Couplings of bending-stretching, shear-stretching, twist-stretching and bending-twisting, depending on lamination scheme affect the critical flutter speed. Flutter boundary increases with increase in aspect ratio and thickness ratio, irrespective of the boundary conditions and ply-orientations studied here. For a deep panel, the transverse boundary conditions and number of layers affect the flutter behaviour qualitatively. It is worthwhile to have experimental investigations for deep (R/b in the range of 1-4) panel.

REFERENCES

1. Dowell, E.H. Panel flutter. A review of aeroelastic stability of plates and shells. *A.I.A.A. J.*, 1970, **8**, 385-99.
2. Dowell, E.H. Nonlinear oscillations of a fluttering plate I. *A.I.A.A. J.*, 1966, **4**, 1267-75.
3. Dowell, E.H. Nonlinear oscillations of a fluttering plate II. *A.I.A.A. J.*, 1967, **5**, 1856-62.

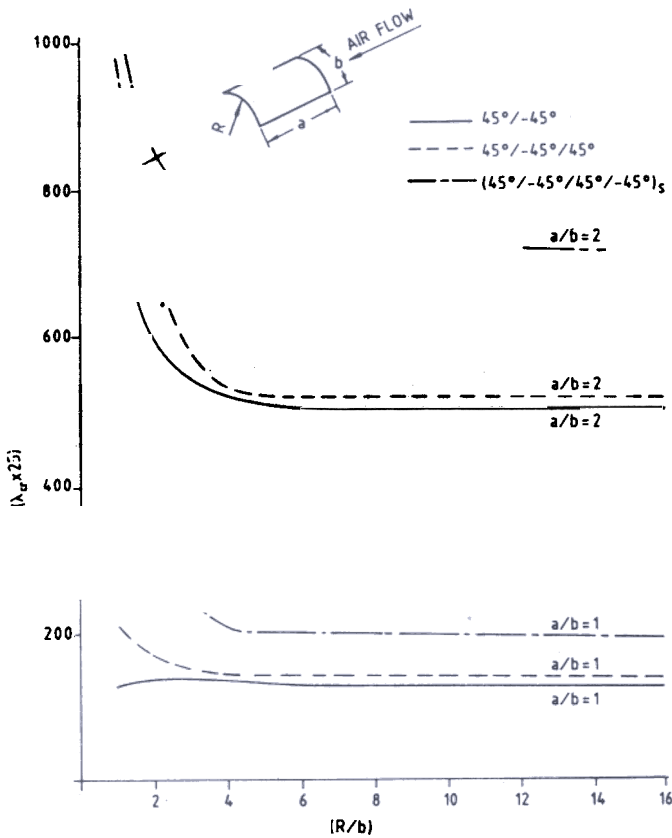


Figure 14. Critical dynamic pressure vs radius-to-side ratio for multilayered angle-ply panels with clamped boundary condition ($b/h = 10$).

4. Morina, L. A perturbation method for treating nonlinear panel flutter problems. *A.I.A.A. J.*, 1969, 7, 405-11.
5. Ventres, C.S. & Dowell, E.H. Comparison of theory and experiment for nonlinear flutter of loaded plates. *A.I.A.A. J.*, 1970, 8, 2022-30.
6. Kuo, C.C.; Morina, L. & Dungundji, J. Perturbation and harmonic balance method for nonlinear panel flutter. *A.I.A.A. J.*, 1972, 10, 1479-84.
- Olson, M.D. Some flutter solutions using finite elements. *A.I.A.A. J.*, 1970, 8, 747-52.
8. Sander, G.; Bon, C. & Gerdin, M. Finite element analysis of supersonic panel flutter. *Int. J. Numer. Methods Engg.*, 1973, 7, 379-94.
9. Chu, Mei. A finite element approach for nonlinear flutter. *A.I.A.A. J.*, 1977, 15, 1107-10.
10. Han, A.D. & Yang, T.Y. Nonlinear panel flutter using high-order triangular finite elements. *A.I.A.A. J.*, 1983, 21, 1453-61.
1. Rao, K.S. & Rao, G.V. Nonlinear supersonic flutter of panels considering shear deformation and rotary inertia. *Comp. Struct.*, 1983, 17, 361-64.
12. Sarma, B.S. & Varadan, T.K. Nonlinear panel flutter by finite element method. *A.I.A.A. J.*, 1987, 5, 566-74.
13. Permutter, A.A. On the aeroelasticity of orthotropic panels in supersonic flows. *J. Aerospace Sci.*, 1962, 29, 1132-38.
14. Calligerous, J.M. & Dungundji, J. Effects of orthotropicity orientation on supersonic panel flutter. *A.I.A.A. J.*, 1963, 1, 2180-82.
15. Bohon, H.L. & Anderson, M.S. Role of boundary conditions on flutter of orthotropic panels. *A.I.A.A. J.*, 1966, 4, 1241-48.
16. Ketter, D.J. Flutter of flat rectangular orthotropic panels. *A.I.A.A. J.*, 1967, 5, 116-24.
17. Sawyer, J.W. Flutter and buckling of general laminated plates. *J. Aircraft*, 1977, 14, 387-93.
18. Birman, V. & Librescu, L. Supersonic flutter of shear deformable laminated composite flat panels. *J. Sound & Vibr.* 1990, 139, 265-75.
19. Srinivasan, R.S. & Babu, B.J.C. Free vibration and flutter of laminated quadrilateral plates. *Comput. Struct.*, 1987, 27, 297-04.
20. Voss, H.M. Effects of an external supersonic flow on vibration characteristics of thin shells. *J. Aerospace Sci.*, 1961, 28, 945-56.
21. Dowell, E.H. Nonlinear flutter of curved plates I. *A.I.A.A. J.*, 1969, 7, 424-31.
22. Dowell, E.H. Nonlinear flutter of curved plates II. *A.I.A.A. J.*, 1970, 8, 259-61.
23. Matsuzaki, Y. Natural vibration and flutter of cylindrically curved panels. *A.I.A.A. J.*, 1973, 11, 771-72.
24. Srinivasan, R.S. & Babu, B.J.C. Flutter of clamped circular cylindrical symmetrically layered panels. *J. Sound & Vibr.* 1990, 142, 532-35.
25. Lin, K.J.; Lu, P.I. & Tarn, J.Q. Flutter analysis of composite panels using high-precision finite elements. *Comput. Struct.*, 1989, 33, 561-74.
26. Leo, I. & Cho, M.H. Finite element analysis of composite panel flutter. *Comput. Struct.*, 1991, 39, 165-72.

27. Shian, L.C. & Chang, J.T. Finite element analysis of supersonic flutter of multi-bay composite panels. *Comput. Struct.*, 1991, **39**, 269-76.
28. Prathap, G.; Naganarayana, B.P. & Somashekar, B.R. Field-consistency analysis of isoparametric eight-noded bending element. *Comput. Struct.*, 1988, **29**, 857-74.
29. Jones, R.M. *Mechanics of composite materials*. McGraw Hill, New York, 1975.
30. Dixon, S.C. Comparison of panel flutter results from approximate aerodynamic theory with results from exact theory and experiment. NASA, Washington DC, NASA TND – 3649.
31. Mei, C. & Rogers Jr. J.L. Application of NASTRAN to large deflection supersonic flutter of panels. NASA, Washington DC, NASA TMX 3428.